

Supporting information

Visual discrimination of aromatic acids substitution patterns by supramolecular nanocooperativity

Mykola Kravets,^a Grzegorz Sobczak,^a Nazar Rad,^a Iwona Misztalewska-Turkowicz,^b Oksana Danylyuk,^a and Volodymyr Sashuk^{a*}

^aInstitute of Physical Chemistry of the Polish Academy of Sciences, Kasprzaka 44/52, 01-224 Warsaw, Poland

^bUniversity of Białystok, Faculty of Chemistry, Ciołkowskiego 1K, 15-245 Białystok, Poland

Experimental Section

General information:

All chemicals were purchased as reagent grade from commercial suppliers and used without further purification. Solvents were of analytical grade quality. Experiments were performed at room temperature unless otherwise noted. Deionized water (18.3 MΩ·cm) was obtained from Milli-Q station. NMR spectra were recorded on a Bruker 400 MHz instrument. NMR data were analyzed using Mnova software. Fitting procedure was performed using HypNMR software. Single crystals were grown by slow evaporation of the solvent from an aqueous solution of P4P and terephthalic acid. X-ray data were collected at 100 K on the SuperNova Agilent diffractometer using CuKα radiation ($\lambda = 1.54184 \text{ \AA}$) and processed with CrysAlisPro. Solution and refinement of the structure were done using the programs integrated in WinGX software system.^[1] Structure was solved by direct methods and refined using SHELXL-2013.^[2] DLS and ξ -potential were measured on Malvern Zetasizer. TEM images were taken with FEI TECNAI and analyzed by ImageJ. SEM images were recorded by FEI Nova NanoSEM 450.

Synthesis of “naked” gold nanoparticles (AuNPs):

To 10 ml of water was added 330 μL of 24.3 mM aqueous HAuCl_4 solution. After 4 minutes stirring to this mixture was added 400 μL of 100 mM freshly prepared aqueous NaBH_4 solution by a single injection. The final solution was stirred for 2 min.

Synthesis of P4P coated gold NPs:

To 100 μL of 39.21 mM aqueous P4P solution, 1200 μL of 0.75 mM AuNPs (in terms of gold atoms) was added portionwise at 200 μL (each portion was added about every 10 s) with constant stirring for 2 min.

Gold NPs covered with TMA ligand were prepared in an analogous manner.

Titration experiments:

To a solution of **P4P** (7.4 mM) in TRIS (50 mM) a solution of 1,2-acid (66.2 mM) and **P4P** (7.4 mM) in TRIS (50 mM) was added portionwise.

¹H NMR spectra were recorded at [acid]/[P4P] = 0.11, 0.22, 0.33, 0.43, 0.53, 0.63, 0.72, 0.82, 0.91, 1.00, 1.09, 1.17, 1.26, 1.34, 1.42, 1.50, 1.58, 1.65, 1.73, 1.80, 1.94, 2.08, 2.20, 2.33, 2.45, 2.6, 2.74., 2.87, 3.00:

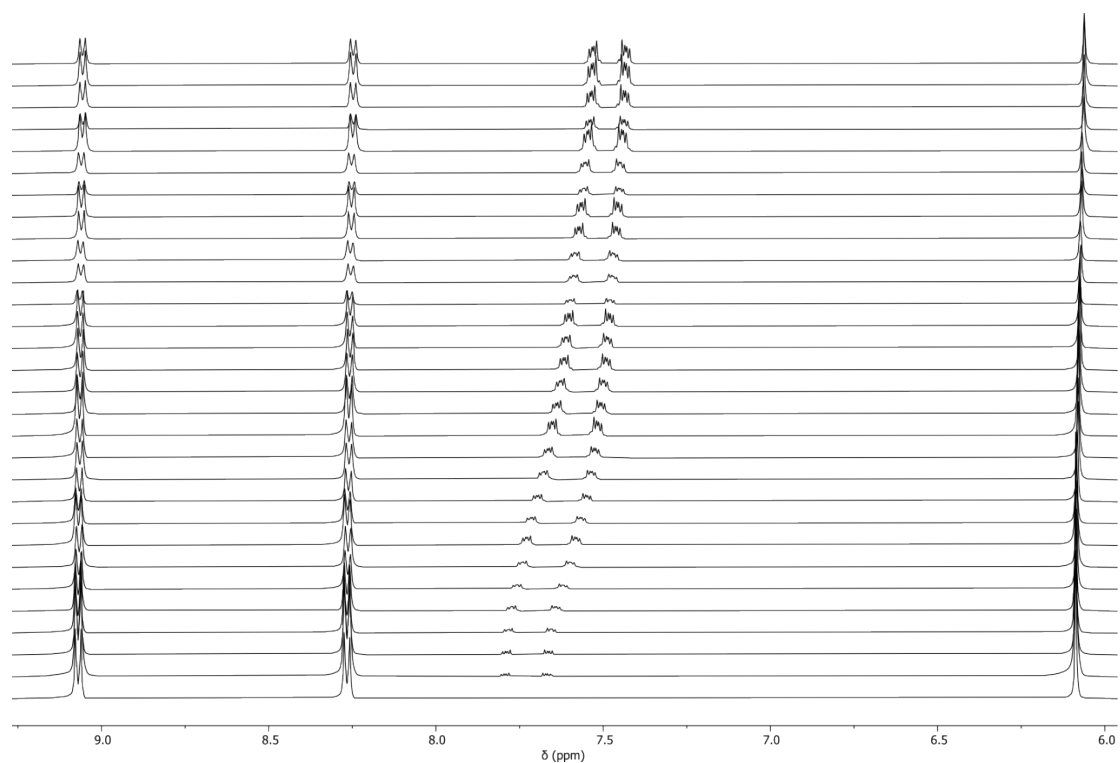


Fig. S1 ^1H NMR spectra of **P4P** with increasing amount of 1,2-acid ((303 K, D_2O)).

To a solution of **P4P** (1.5 mM) in TRIS (10 mM) a solution of 1,3-acid (13.2 mM) and **P4P** (1.5 mM) in TRIS (10 mM) was added portionwise.

^1H NMR spectra were recorded at [acid]/[P4P] = 0.11, 0.22, 0.33, 0.43, 0.53, 0.63, 0.72, 0.82, 0.91, 1.00, 1.09, 1.17, 1.26, 1.34, 1.42, 1.50, 1.58, 1.65, 1.73, 1.80, 1.94, 2.08, 2.20, 2.33, 2.45, 2.6, 2.74:

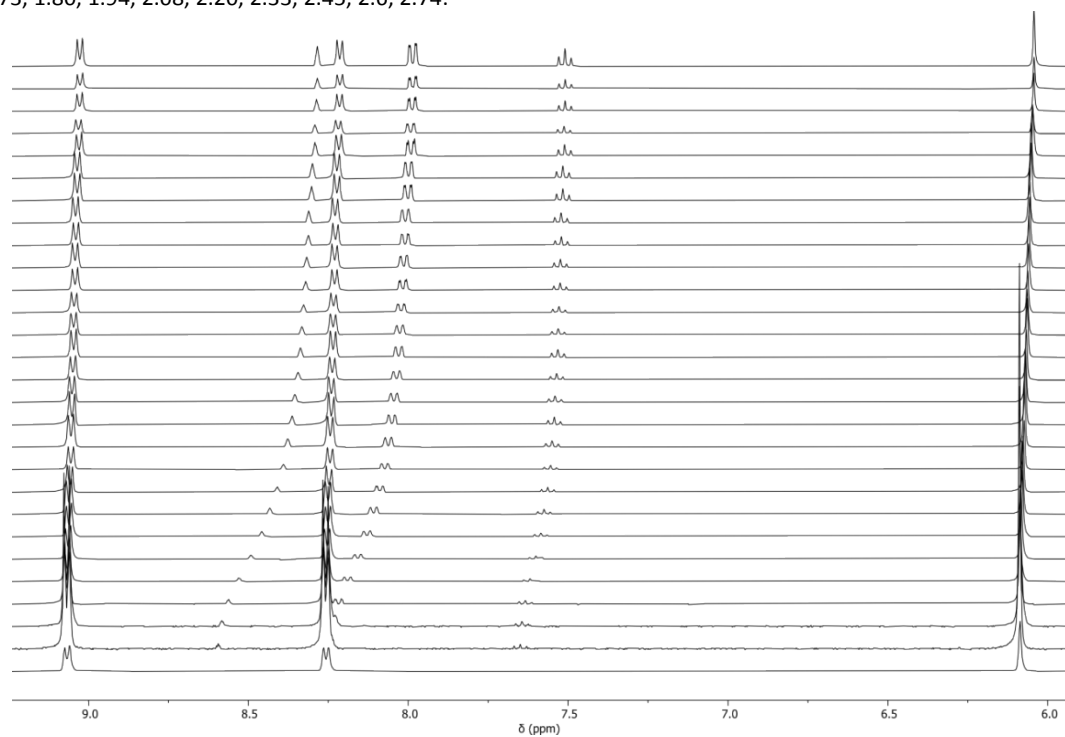


Fig. S2 ^1H NMR spectra of **P4P** with increasing amount of 1,3-acid (303 K, D_2O).

To a solution of **P4P** (1.0 mM) in TRIS (6.7 mM) a solution of 1,4-acid (8.8 mM) and **P4P** (1 mM) in TRIS (6.7 mM) was added portionwise.

^1H NMR spectra were recorded at [acid]/[P4P] = 0.11, 0.22, 0.33, 0.43, 0.53, 0.63, 0.72, 0.82, 0.91, 1.00, 1.09, 1.17, 1.26, 1.34, 1.42, 1.50, 1.58, 1.65, 1.73, 1.80, 1.94, 2.08, 2.20, 2.33, 2.45, 2.6, 2.74, 2.87:

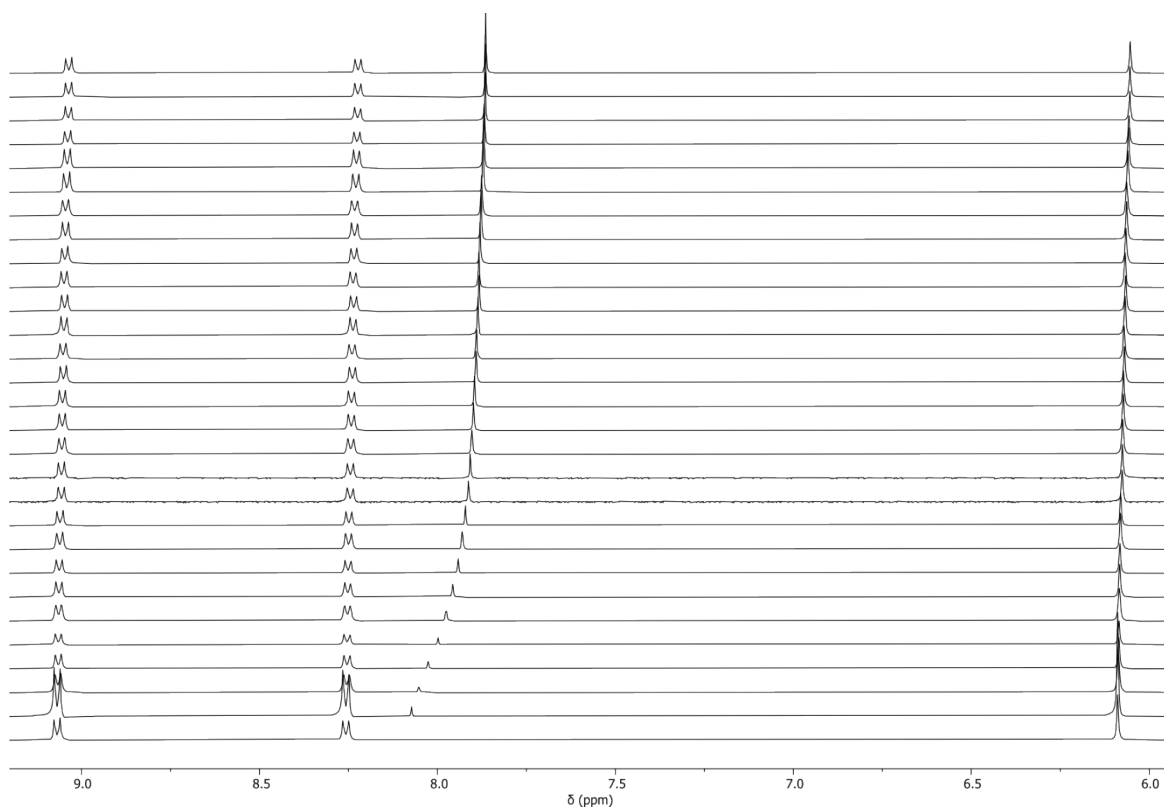


Fig. S3 ^1H NMR spectra of **P4P** with increasing amount of 1,4-acid (303 K, D_2O).

The obtained titration points were fitted to different models, as presented below. For single [HG] and mixed [HG, HG2], [HG, H2G] models, substantial deviations in non-linear curve fitting were observed. The best fit we obtained for the models comprising three kinds of complexes (HG, HG2, H2G).

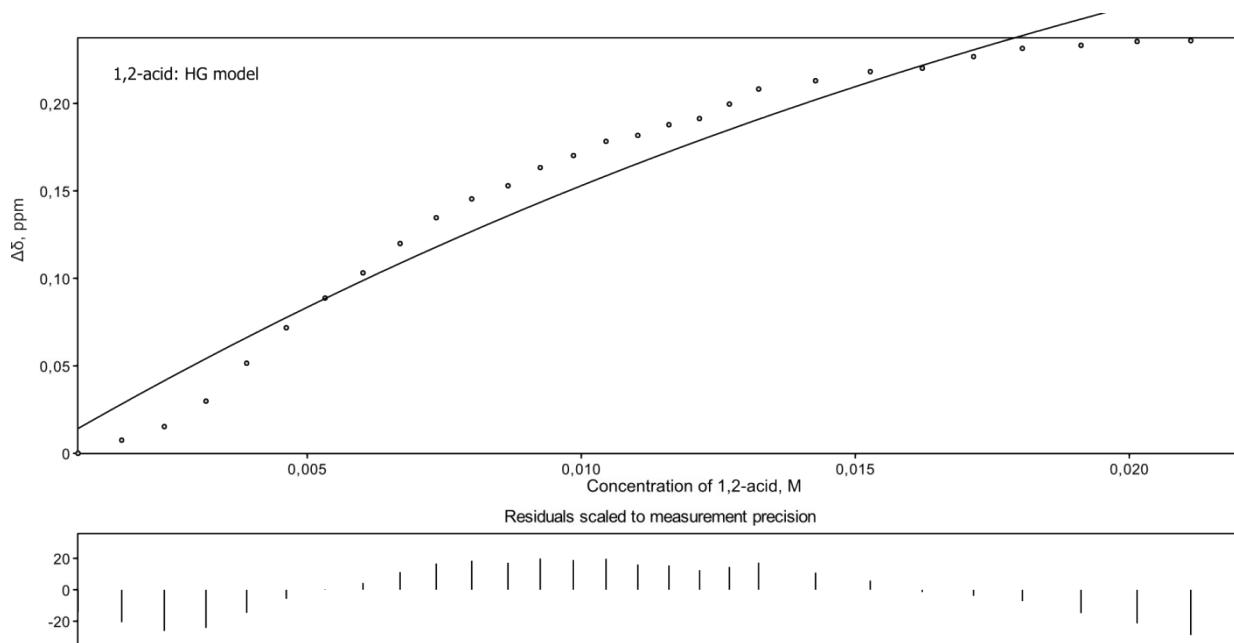


Fig. S4 Non-linear curve fitting and the residual plot.

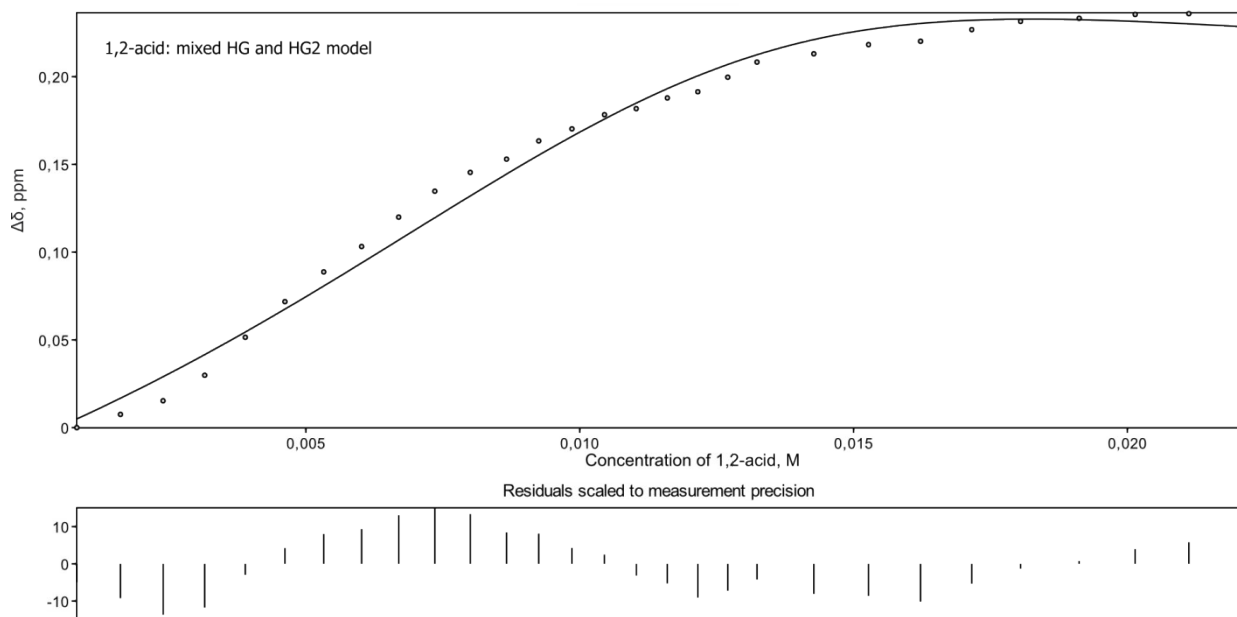


Fig. S5 Non-linear curve fitting and the residual plot.

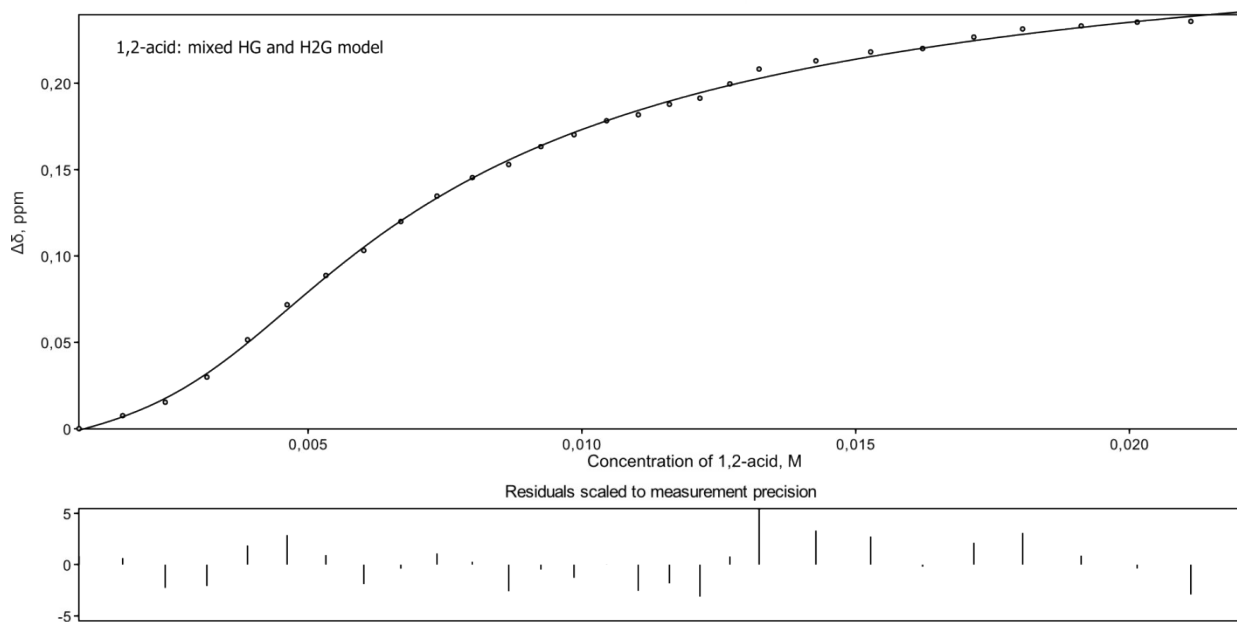


Fig. S6 Non-linear curve fitting and the residual plot.

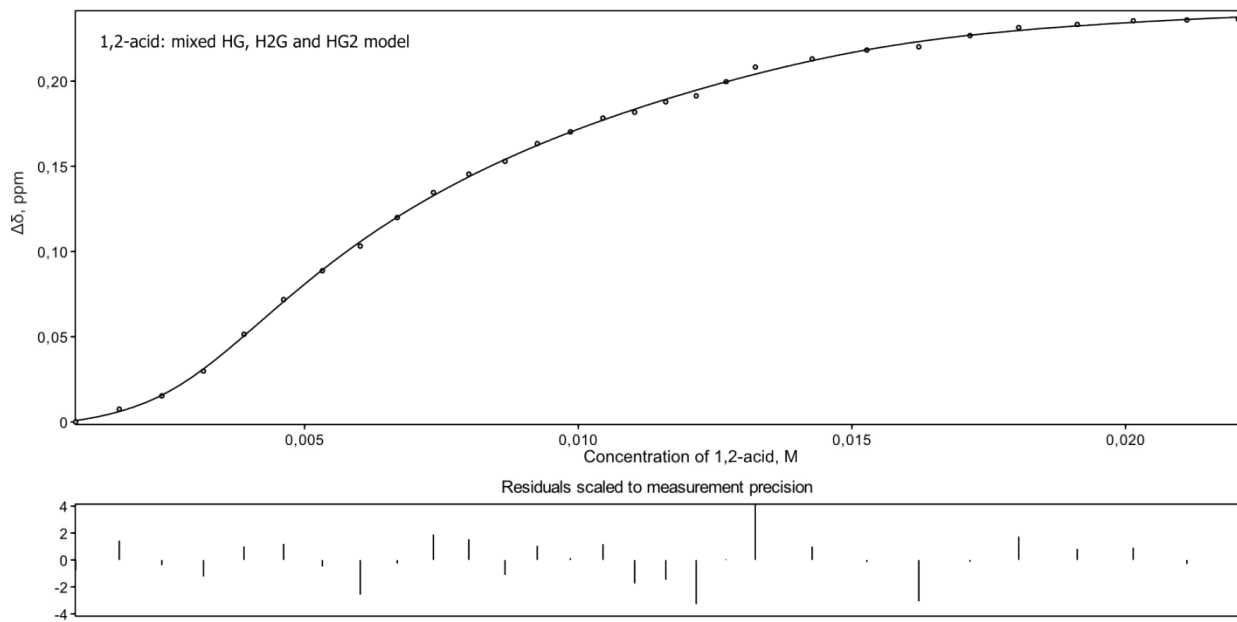


Fig. S7 Non-linear curve fitting and the residual plot.

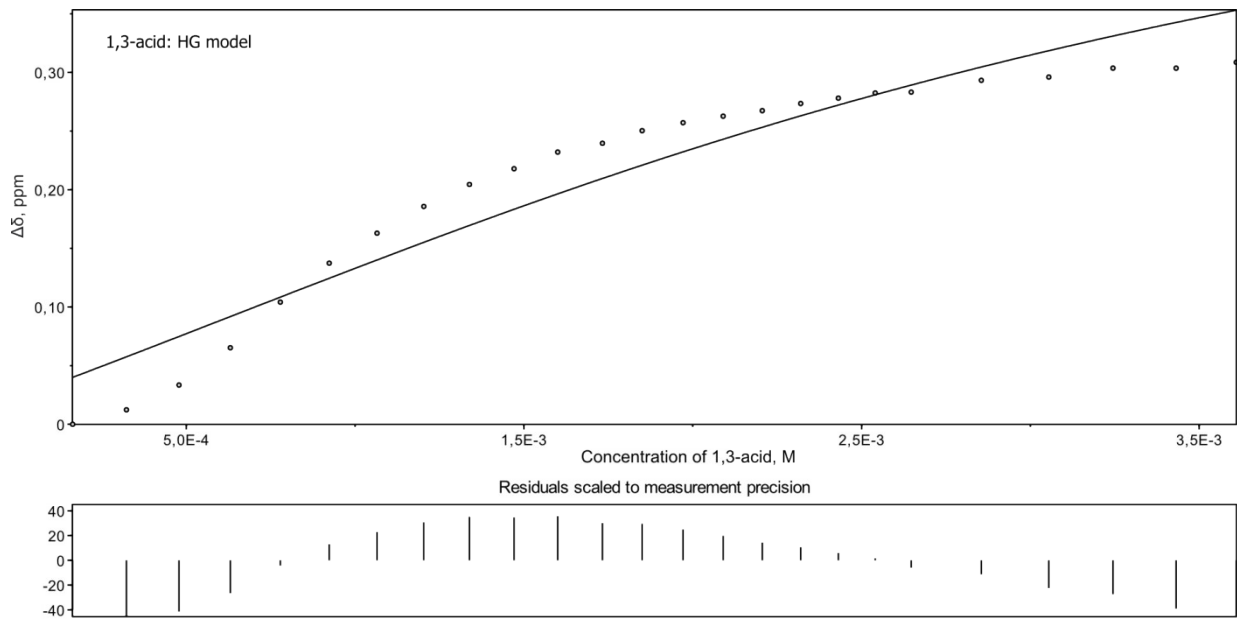


Fig. S8 Non-linear curve fitting and the residual plot.

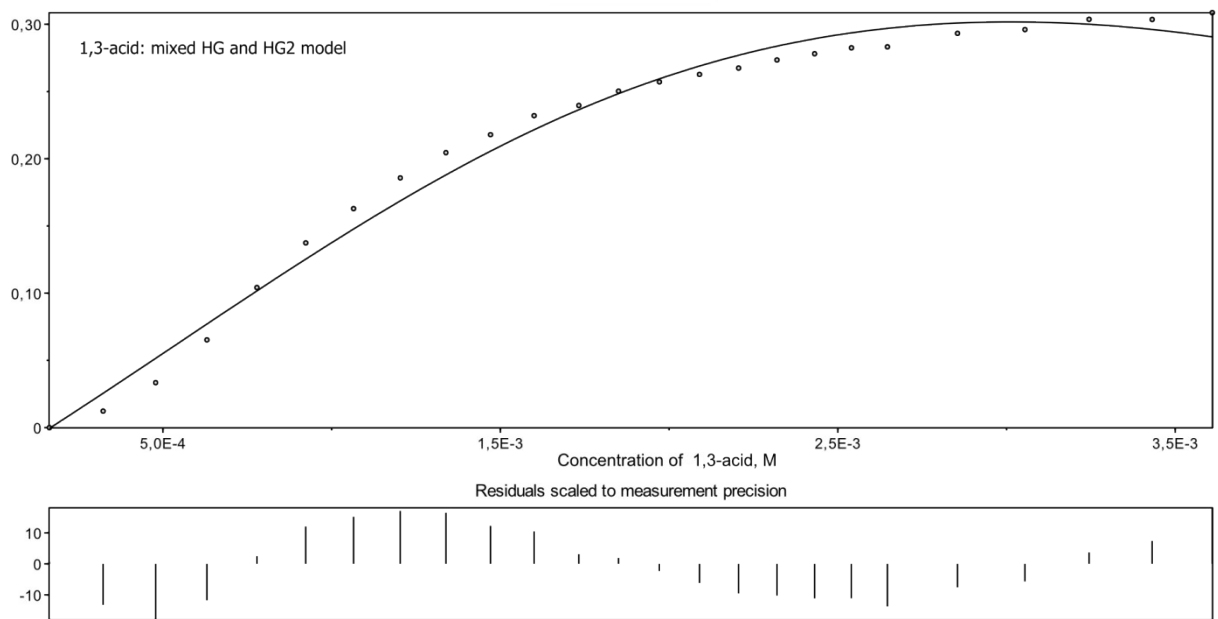


Fig. S9 Non-linear curve fitting and the residual plot.

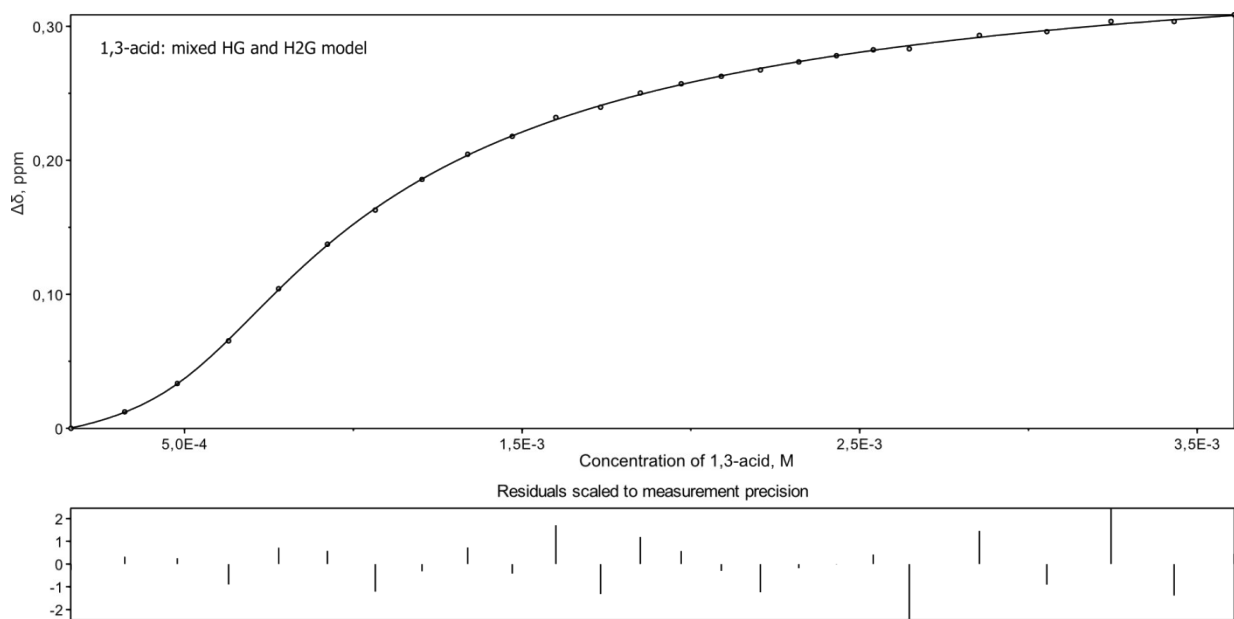


Fig. S10 Non-linear curve fitting and the residual plot.

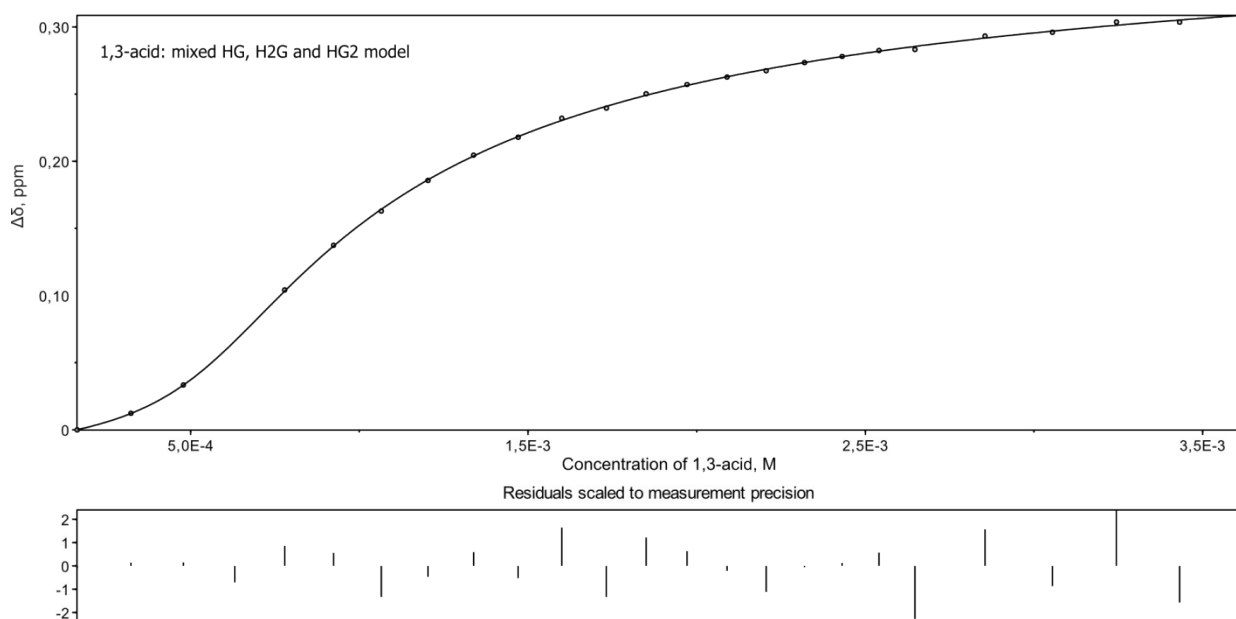


Fig. S11 Non-linear curve fitting and the residual plot.

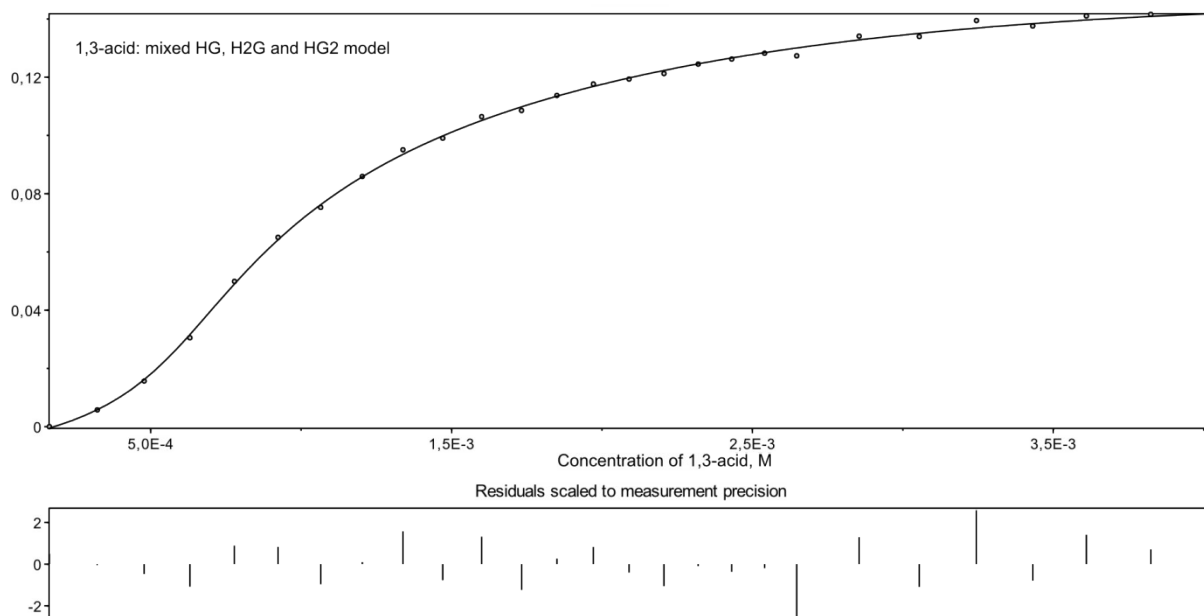


Fig. S12 Non-linear curve global fitting (on three proton signals) and the residual plot.

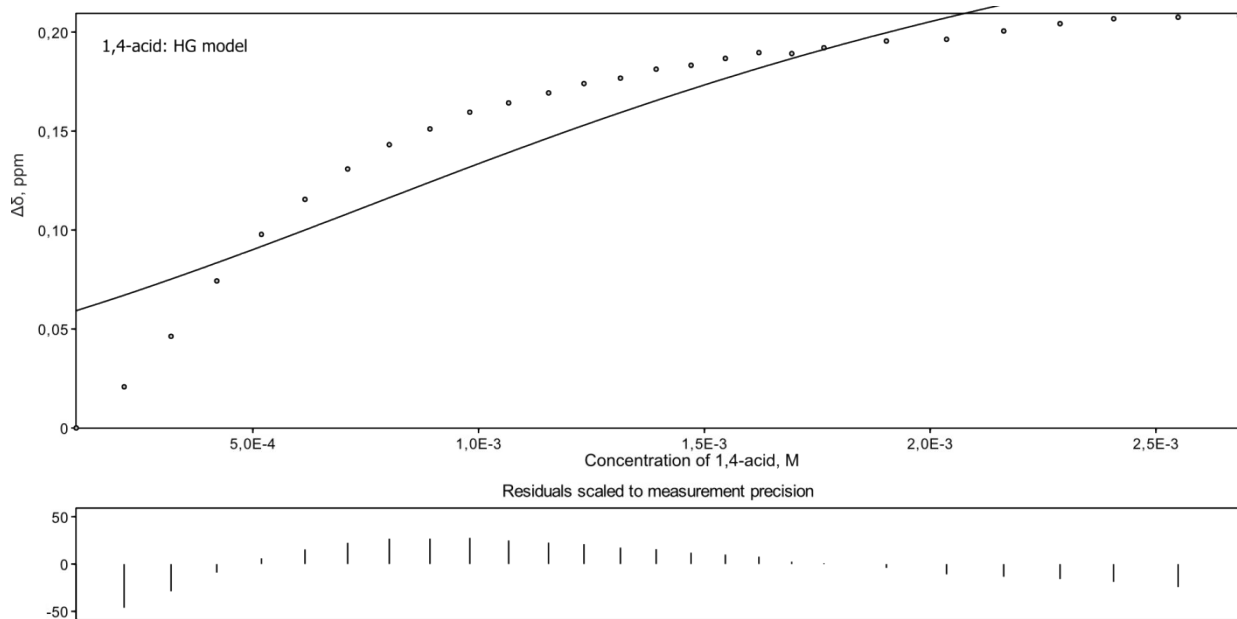


Fig. S13 Non-linear curve fitting and the residual plot.

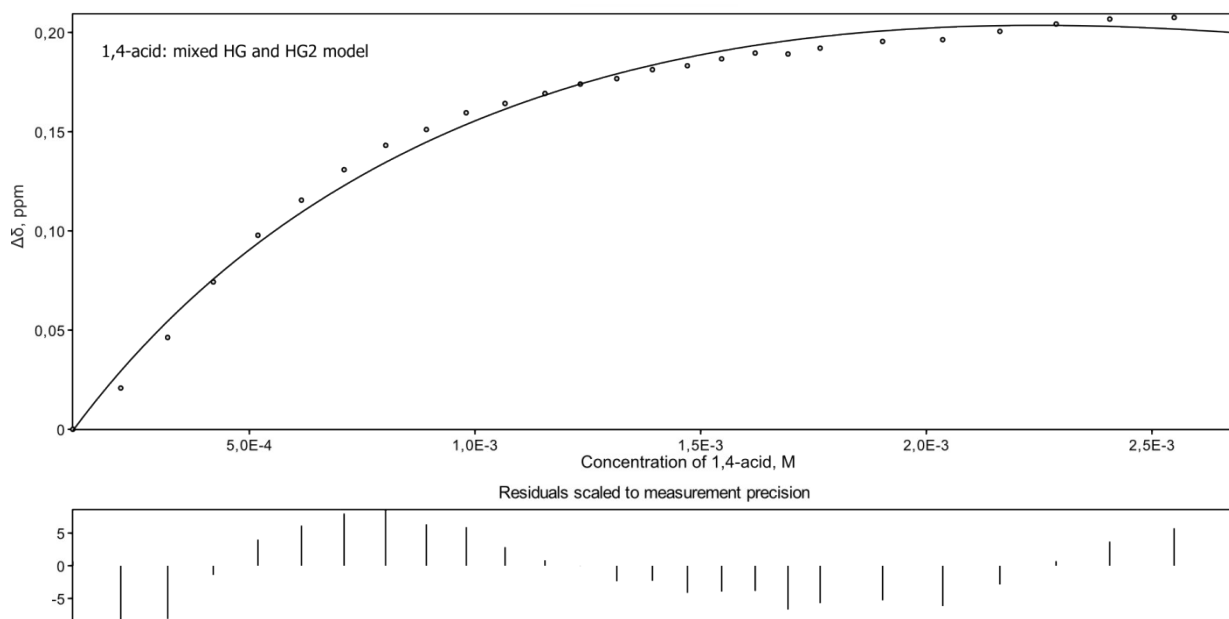


Fig. S14 Non-linear curve fitting and the residual plot.

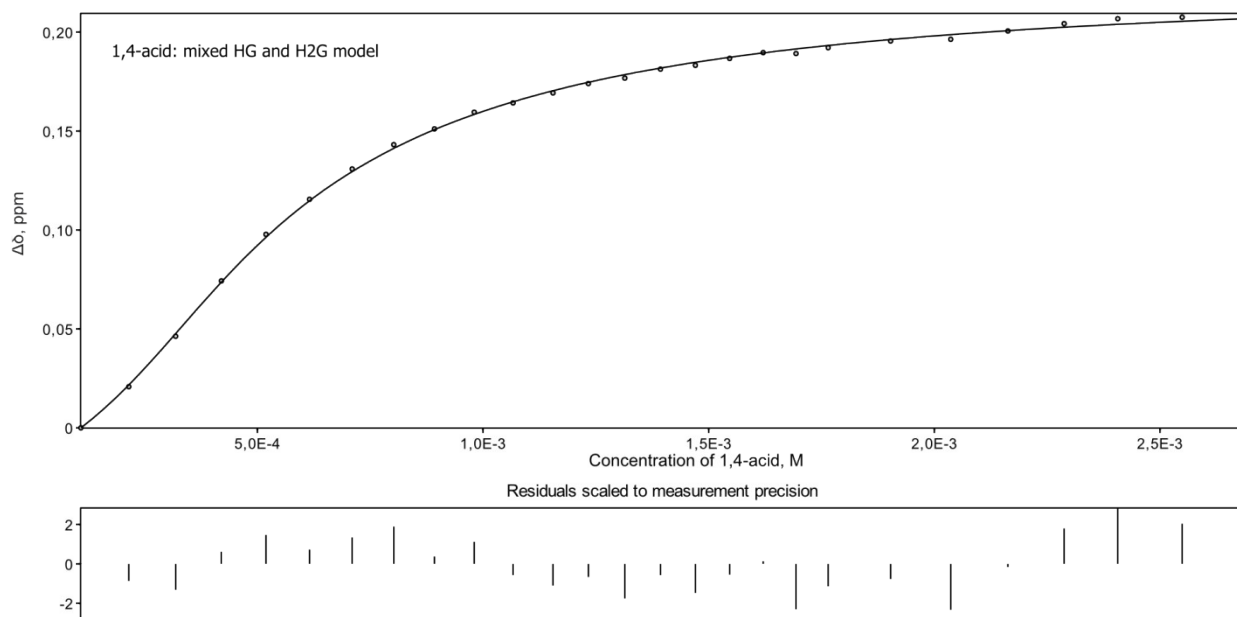


Fig. S15 Non-linear curve fitting and the residual plot.

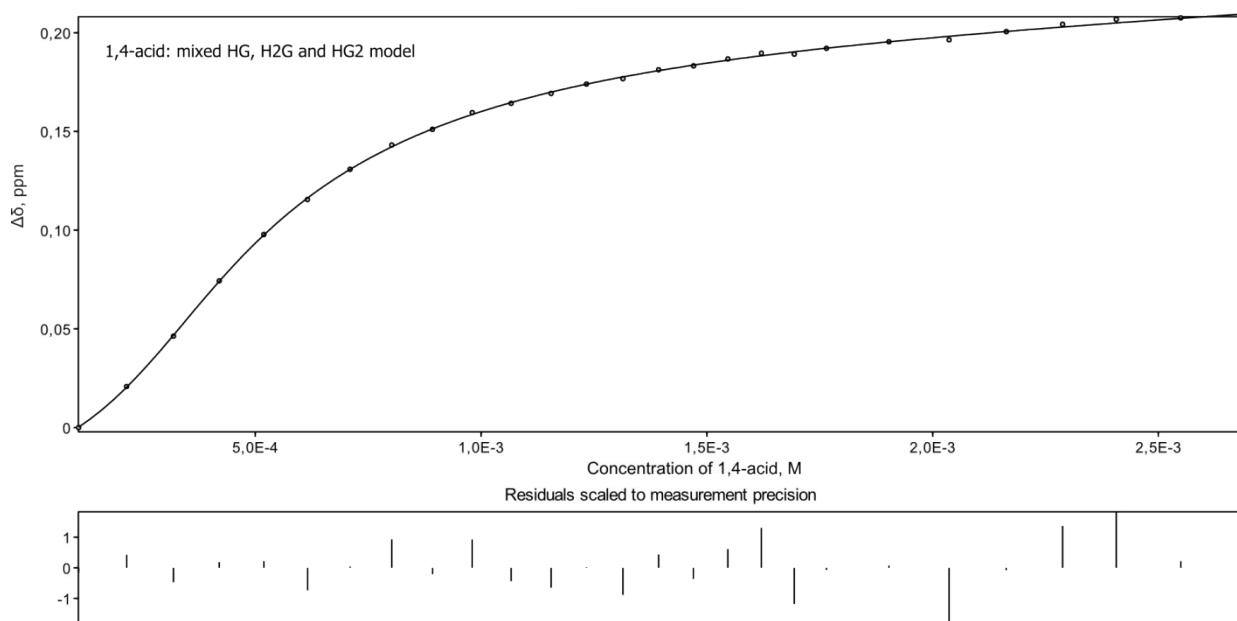


Fig. S16 Non-linear curve fitting and the residual plot.

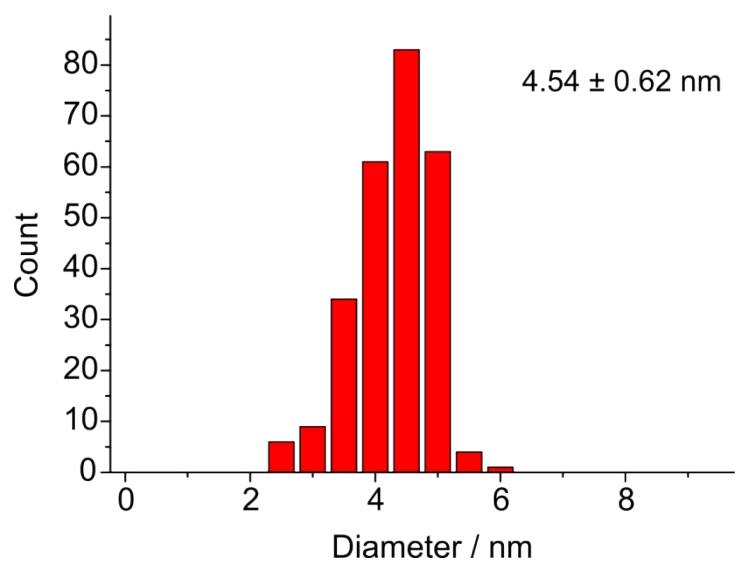


Fig. S17 Particle size distribution for gold nanoparticles determined from TEM images.

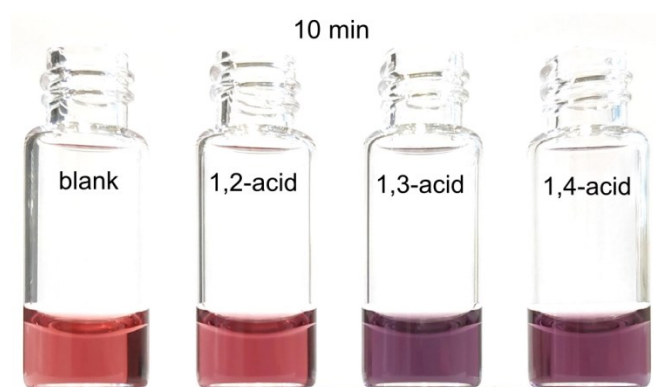


Fig. S18 Photograph of glass vials filled with **P4P** coated gold NPs taken 10 minutes after mixing with phthalic acids.

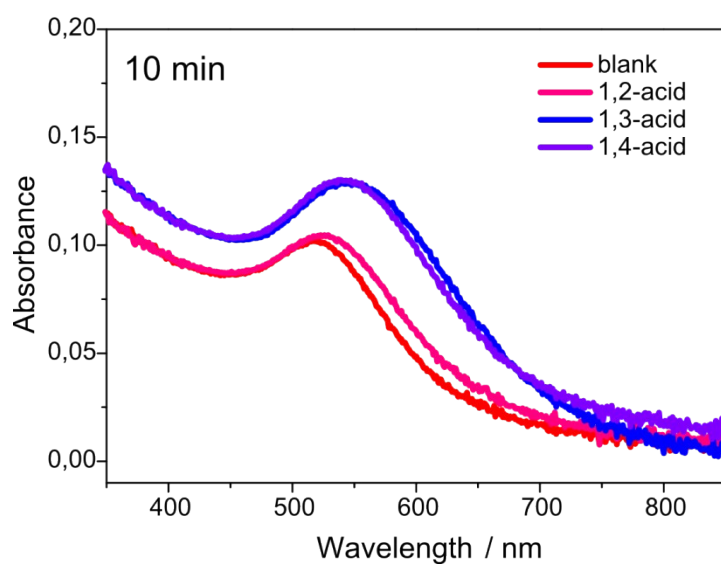


Fig. S19 UV-Vis spectra of **P4P** coated gold NPs taken 10 minutes after mixing with phthalic acids.

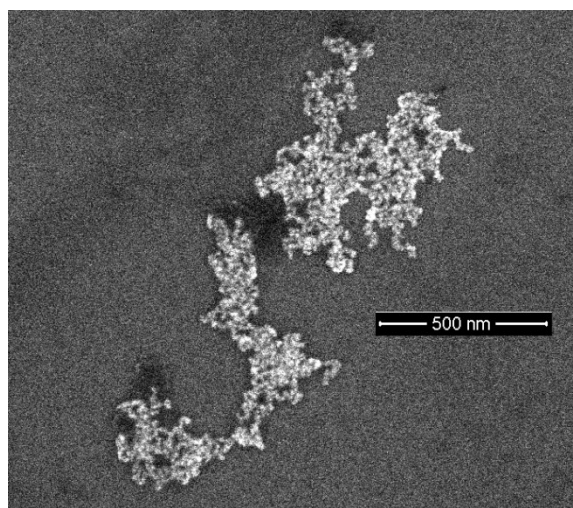


Fig. S20 SEM image of **P4P** coated gold NPs mixed with 1,3-acid.

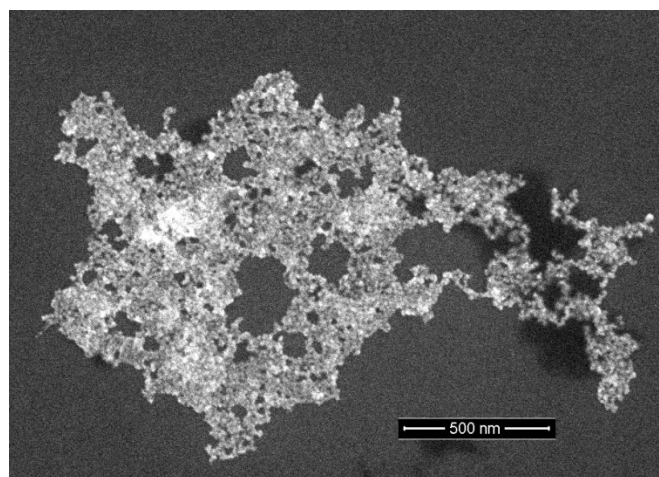


Fig. S21 SEM image of **P4P** coated gold NPs mixed with 1,4-acid.

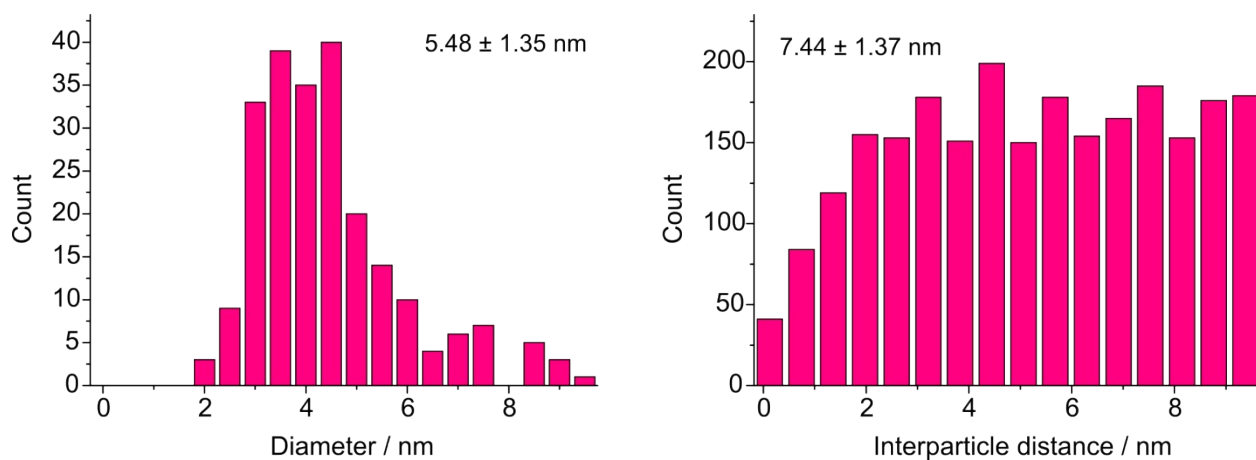


Fig. S22 Histograms of particle size (left) and center-to-center interparticle distance (right) distributions for **P4P** coated gold NPs mixed with 1,2-acid. Surface-to-surface distance was calculated as the difference between them.

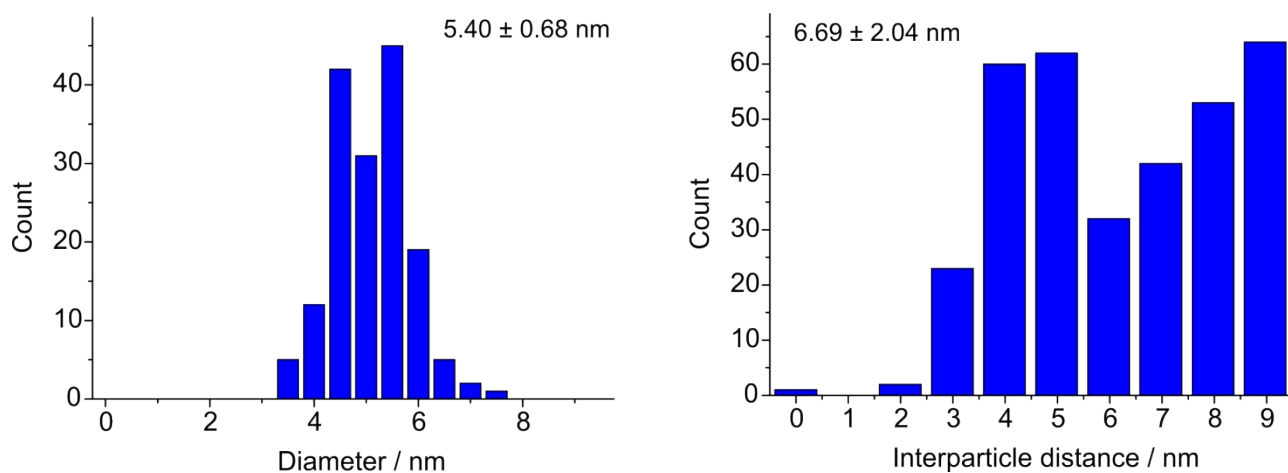


Fig. S23 Histograms of particle size (left) and center-to-center interparticle distance (right) distributions for **P4P** coated gold NPs mixed with 1,3-acid. Surface-to-surface distance was calculated as the difference between them.

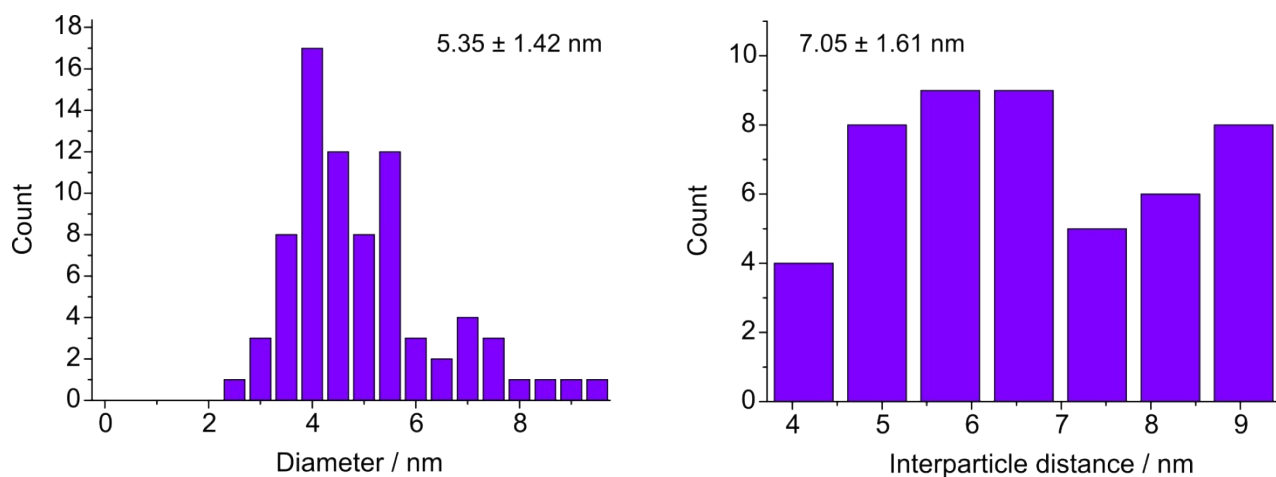


Fig. S24 Histograms of particle size (left) and center-to-center interparticle distance (right) distributions for **P4P** coated gold NPs mixed with 1,4-acid. Surface-to-surface distance was calculated as the difference between them.

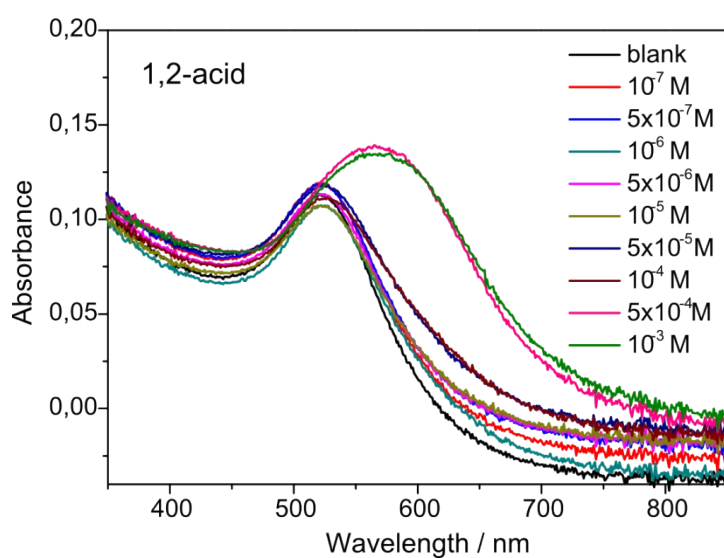


Fig. S25 UV-Vis spectra of **P4P** coated gold NPs with increasing amount of 1,2-acid. The emergence of a new plasmon band is clearly seen at 5×10^{-5} M.

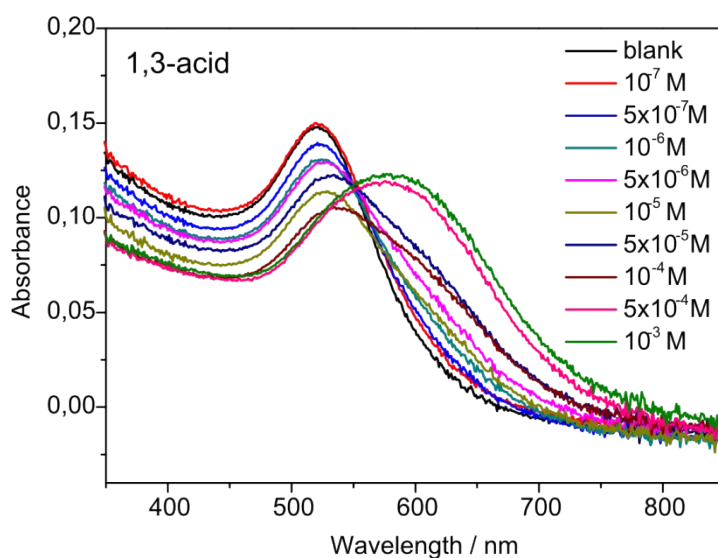


Fig. S26 UV-Vis spectra of P4P coated gold NPs with increasing amount of 1,3-acid. The emergence of a new plasmon band is clearly seen at 1×10^{-6} M.

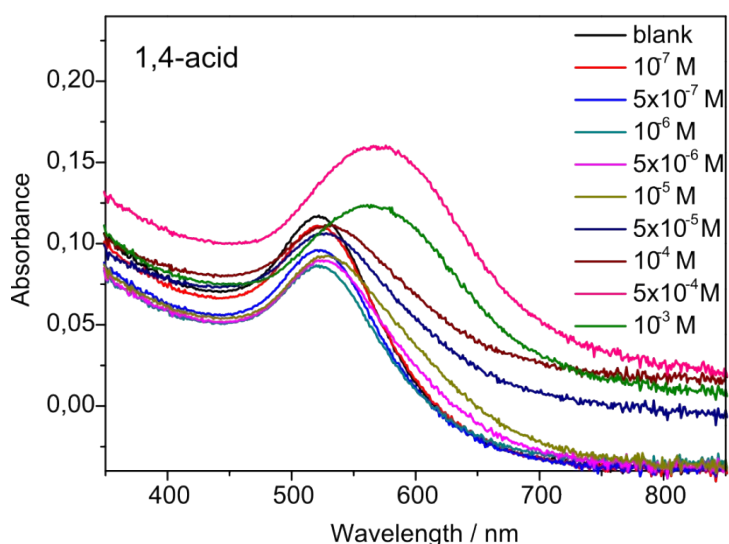


Fig. S27 UV-Vis spectra of P4P coated gold NPs with increasing amount of 1,4-acid. The emergence of a new plasmon band is clearly seen at 5×10^{-6} M.

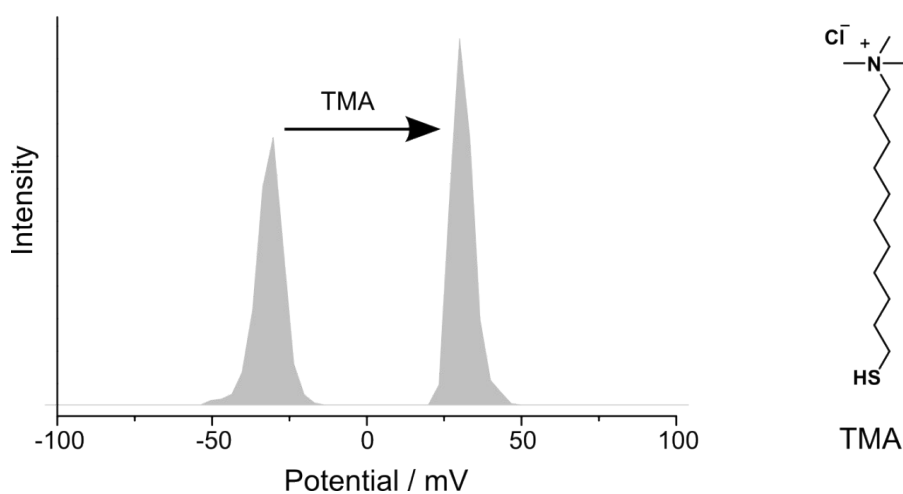


Fig. S28 Change of ξ -potential of a freshly obtained gold sol containing “naked” AuNPs after the addition of TMA.



Fig. S29 Photograph of glass vials filled with **TMA** coated gold NPs taken 10 min after mixing with phthalic acids.



Fig. S30 Photograph of glass vials filled with **TMA** coated gold NPs taken one hour after mixing with phthalic acids.

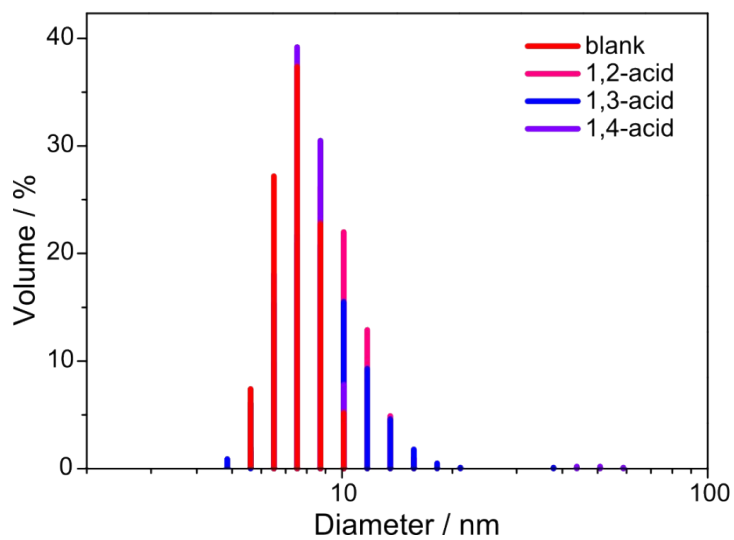


Fig. S31 Particle size distributions for **TMA** coated gold NPs measured by dynamic light scattering one hour after mixing with phthalic acids.

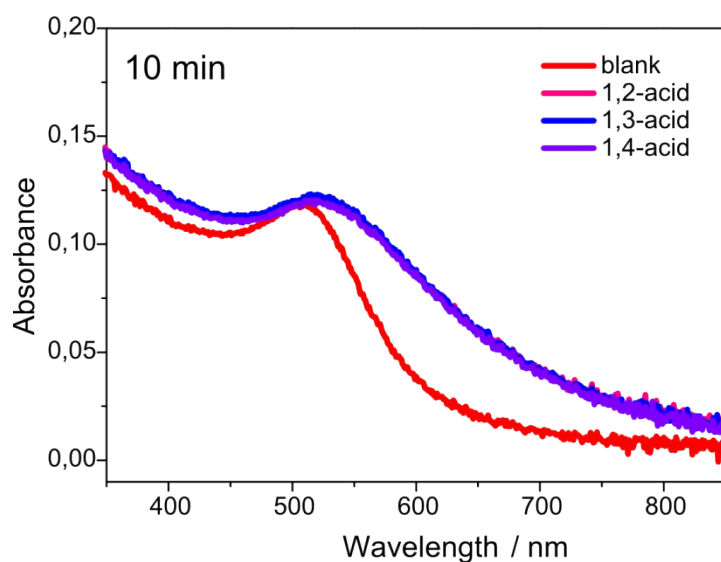


Fig. S32 UV-Vis spectra of **TMA** coated gold NPs taken 10 minutes after mixing with phthalic acids.

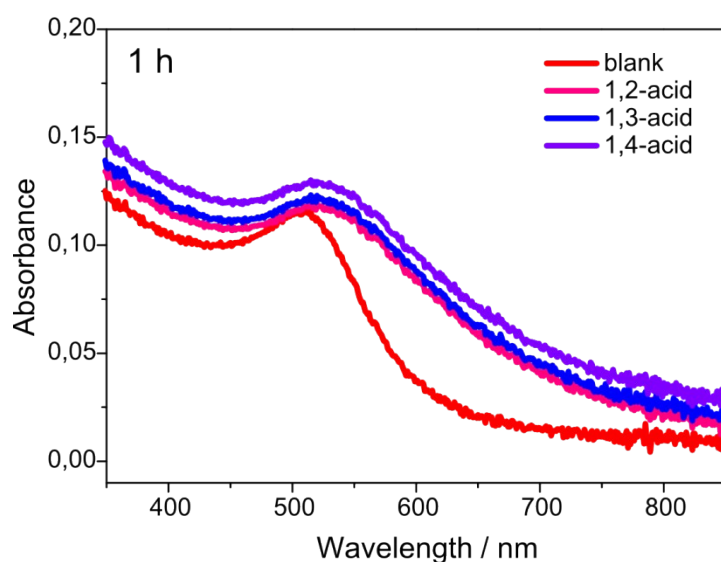


Fig. S33 UV-Vis spectra of **TMA** coated gold NPs taken one hour after mixing with phthalic acids.

Literature:

- [1] L. Farrugia, *J. Appl. Crystallogr.* **2012**, *45*, 849-854.
 [2] G. Sheldrick, *Acta Crystallogr. A* **2008**, *64*, 112-122.